

Adsorption of cesium on different types of activated carbon

Peer-reviewed author version

VANDERHEYDEN, Sara; Van Ammel, R.; Sobiech-Matura, K.; VANREPPELEN, Kenny; SCHREURS, Sonja; SCHROEYERS, Wouter; YPERMAN, Jan & CARLEER, Robert (2016) Adsorption of cesium on different types of activated carbon. In: JOURNAL OF RADIOANALYTICAL AND NUCLEAR CHEMISTRY, 310(1), p. 301-310.

DOI: 10.1007/s10967-016-4807-4

Handle: <http://hdl.handle.net/1942/22713>

1

## **Title page**

2 Names of the authors: S. R. H. Vanderheyden<sup>1</sup>, R. Van Ammel<sup>2</sup>, K. Sobiech-Matura<sup>2</sup>, K.  
3 Vanreppelen<sup>1,3</sup>, S. Schreurs<sup>3</sup>, W. Schroeyers<sup>3</sup>, J. Yperman<sup>1</sup>, R. Carleer<sup>1</sup>

4 Title: Adsorption of cesium on different types of activated carbon

5 Affiliation(s) and address(es) of the author(s):

6 <sup>1</sup>Research Group of Analytical and Applied Chemistry, CMK, Hasselt University,  
7 Diepenbeek, Belgium

8 <sup>2</sup>European Commission, Joint Research Centre, Institute for Reference Materials and  
9 Measurements, Geel, Belgium

10 <sup>3</sup>Research Group of Nuclear Technology, CMK, Hasselt University, Diepenbeek, Belgium

11 E-mail address of the corresponding author: sara.vanderheyden@uhasselt.be

12



- 36 Environmental remediation
- 37 Low-level (radioactive) waste

## 38 **1. Introduction**

39 Produced only by anthropogenic sources, radioactive Cs isotopes are released into the  
40 biosphere by weapons testing, nuclear reactor accidents and controlled release into waste  
41 water streams. These releases combined with its relatively long half-life ( $T_{1/2} \approx 30$  years),  
42 makes  $^{137}\text{Cs}$  the major contributor to the long term environmental radiation dose received  
43 by humans and other organisms [1]. During the nuclear accident at the Fukushima nuclear  
44 power plant, the estimated release of  $^{137}\text{Cs}$  into the environment amounted to more than 12  
45  $10^{15}$  Bq. Additionally, the short-lived  $^{134}\text{Cs}$  ( $>12 \cdot 10^{15}$  Bq,  $T_{1/2} \approx 2$  years) and  $^{136}\text{Cs}$  ( $>2 \cdot 10^{15}$   
46 Bq,  $T_{1/2} \approx 13$  days) were also released, raising the level of activity in the drinking water  
47 above the legally permitted levels in the nearby areas [2,3]. One estimates that these  
48 atmospheric releases are only a fraction of the releases from the Chernobyl nuclear power  
49 plant during the accident in 1986 [2]. The activity of Cs radioisotopes poses a radiotoxicity  
50 risk caused by external radiation exposure and internal radiation damage after inhalation  
51 of contaminated air or intake of contaminated food or water [4,5]. However, stable Cs in  
52 these concentrations is not known to be harmful. Cs is very mobile in aqueous  
53 environments because of its high solubility, but it strongly binds to soils and minerals. This  
54 promotes accumulation of Cs radioisotopes and contamination of the food chain [5,4,6].  
55 Treatment of radioactive waste water contaminated with Cs isotopes is a challenging  
56 research area in environmental radiation protection [7].

57 Recently, a wide range of low-cost adsorbents were investigated for the removal of Cs from  
58 wastewater because other methods such as chelation and precipitation are rather ineffective  
59 for the removal of trace amounts of Cs [8-10]. Studies have been carried out using different  
60 organic and inorganic ion exchangers, such as Prussian blue (PB) and other  
61 hexacyanoferrates (HCF) [11-13]. HCFs have a major disadvantage: they exist mainly as  
62 micro-particles (particle diameter  $<100$  nm). These micro-particles are hard to filtrate from  
63 aqueous solutions and can clog a fixed bed reactor causing a significant pressure loss.  
64 Recent research has shown that adsorption of cesium is a promising remediation method

65 for contaminated liquid wastes, if the operating costs can be kept sufficiently low [7,14,15].  
66 Combining HCF (nano)particles with a carrier material having beneficial characteristics  
67 could provide a practical and efficient material for Cs removal [9,12,16,17]. Incorporation  
68 of HCF on biosorbents provides a solution for the filtration problems associated with  
69 unbound HCF [9,17]. The incorporation of these HCF in a porous material would lead to  
70 an increased amount of HCF for a specific volume, thereby increasing adsorption  
71 efficiency.

72 Activated carbon (AC), having high surface area and developed porosity is a low-cost and  
73 effective adsorbent for a wide range of pollutants [18,19]. AC has been used in research to  
74 remove radionuclides from waste water solutions in a relatively straightforward way  
75 compared to other methods [20]. AC has multiple surface functionalities, a high  
76 mechanical strength and a good resistance towards chemicals, heat and radiation [19,21].  
77 Most of the AC produced presently is made by steam activation of mined coal. However,  
78 it might be economically interesting to produce AC from biomass by pyrolysis, followed  
79 by chemical or physical activation. During physical activation, a carbonised biomass is  
80 treated with a mildly oxidising gas at 750 – 900 °C to increase its porosity and surface area  
81 [18,22-25]. Carbonisation and activation of biomass has previously proven to produce  
82 economically valuable AC, if the source material has a consistent and lignin-rich  
83 composition [19,26-28]. Brewers spent grain (BSG) is an interesting source material for  
84 the preparation of AC because of its availability and high nitrogen content. This creates an  
85 in-situ nitrogenised AC, characterised by an increased amount of pyrrolic and pyridinic  
86 surface groups [29,30,27,31]. Because of changed acidic/basic surface characteristics and  
87 a more pronounced chemisorption mechanism, nitrogenised ACs have shown an improved  
88 adsorption towards multiple pollutants compared to normal AC [32-37]. Adsorption of Cs  
89 on ACs has been researched in the past, but with relatively high concentrations of Cs,  
90 generally 10 mg/L and higher [7,38,39].

91 In order to find an AC suitable for Cs removal from waste water, adsorption capacities for  
92 lower Cs concentrations are measured and presented in this paper. Furthermore, a simple  
93 HCF incorporation on the surface of the AC is tested, in order to find a synergistic effect  
94 between adsorption and the HCF ion exchangers. Focussing on low concentrations of Cs  
95 and different adsorption techniques, adsorption capacities are compared for different types

96 of AC. A series of experiments was set up for the study in order to investigate the key  
97 adsorption parameters. This could provide good tools for future low-level adsorption  
98 experiments.

## 99 **2. Experimental**

100 The goal of this experiment was to study and optimise the removal of Cs from water using  
101 different ACs. To study the behaviour of the Cs,  $^{134}\text{Cs}$  was used as a tracer. A standard Cs  
102 solution was irradiated to activate a fraction of the stable Cs to  $^{134}\text{Cs}$ . The  $^{134}\text{Cs}$  solution  
103 was brought in contact with AC under different experimental conditions. In this experiment  
104 the optimal settings for adsorption were tested by varying the AC, the pH and the  
105 adsorption technique.

106 Three adsorption techniques were evaluated: batch adsorption tests and two types of  
107 column tests. Batch adsorption tests were based on the equilibrium between the AC  
108 adsorbents (5 different types plus their modified form) and the Cs solution after 48 hours  
109 of shaking. Column adsorption tests resembled industrial adsorption filter systems and can  
110 be performed in two ways. Firstly, a single column containing the AC can be used multiple  
111 times to extract Cs from the same solution, until saturation of the AC surface is reached.  
112 This is referred to later on as a ‘single column’ experiment and is conducted with the 5  
113 ACs. Secondly, a solution can be filtered through different sequential columns to remove  
114 Cs. This is referred to as ‘sequential column’ experiment and was performed only for Norit  
115 GAC 1240.

116 To prepare the solutions needed in the experiments, Milli-Q/Nanopure water and analytical  
117 grade reagents were used. All labware was cleaned with detergent and water prior to use.  
118 Glassware, centrifuge tubes and filtration columns were filled with a solution containing  
119  $20\text{ mg L}^{-1}$  of stable Cs having the same pH as the solution used in the experiments and left  
120 overnight in order to saturate their surfaces with stable Cs.

### 121 **2.1 Activated carbon**

122 Five different types of AC were used in the experiments. Three of them were prepared from  
123 BSG using a custom made pyrolysis/activation reactor as described previously in [27].  
124 BSG was dried at  $105 \pm 5\text{ }^\circ\text{C}$  for 24 h and sieved to obtain a particle size smaller than 2

125 mm. These three ACs were prepared at different temperatures, using different steam  
 126 activation durations and quantities of Milli-Q water: ACBSG05 (800 °C/30 min/10 mL),  
 127 ACBSG06 (850 °C/45 min/15 mL) and ACBSG07 (800 °C/45 min/15 mL). For  
 128 comparison, the two most widely used commercially available ACs were used: Norit GAC  
 129 1240 (Cabot Corporation, Massachusetts, USA) and Filtrasorb400 (Chemviron Carbon,  
 130 Seneffe, Belgium). Both of these ACs are made from steam-activated bituminous coal and  
 131 have a more mesoporous structure. Their properties make them ideal for removal of a range  
 132 of pollutants from waste water [40,41].

133 An important characteristic of AC is the point of zero charge ( $pH_{PZC}$ ) as it determines at  
 134 which pH the total surface charge of the AC is zero. A pH above the  $pH_{PZC}$  will cause the  
 135 surface of the AC to be negatively charged, attracting the Cs cations to its surface. Solutions  
 136 having  $pH > pH_{PZC}$  will be tested to evaluate the influence of this attraction on adsorption.  
 137 The characteristics of the porosity of the AC were determined by analysis of the BET  
 138 (Brunauer-Emmet-Teller) surface areas (total surface area  $S_{BET}$ , microporous surface area  
 139  $S_{micro}$  and exterior surface area  $S_{ext}$ ), total porosity volume ( $V_T$ ), micropore volume ( $V_{Micro}$ )  
 140 and mesopore volume ( $V_{Meso}$ ) by nitrogen (77 K) adsorption using an Autosorb AS-1  
 141 (Quantachrome, Düsseldorf, Germany) [42,43]. The micropores are characterised by the  
 142 Dubinin – Radushkevich method (volume micropores  $V_{Micro}$ ) and the t-plot method using  
 143 the De Boer method (micropore surface  $S_{micro}$  and extremal surface  $S_{ext}$ ). Before analysis  
 144 the samples were outgassed for 16 h at 200 °C in high vacuum. Experiments were  
 145 performed by ‘Department of Chemistry’, Laboratory for Adsorption and Catalysis,  
 146 University Antwerp, Belgium.

147 **Table 1** BET surfaces and pore volumes of the used ACs determined by nitrogen  
 148 adsorption at 77 K

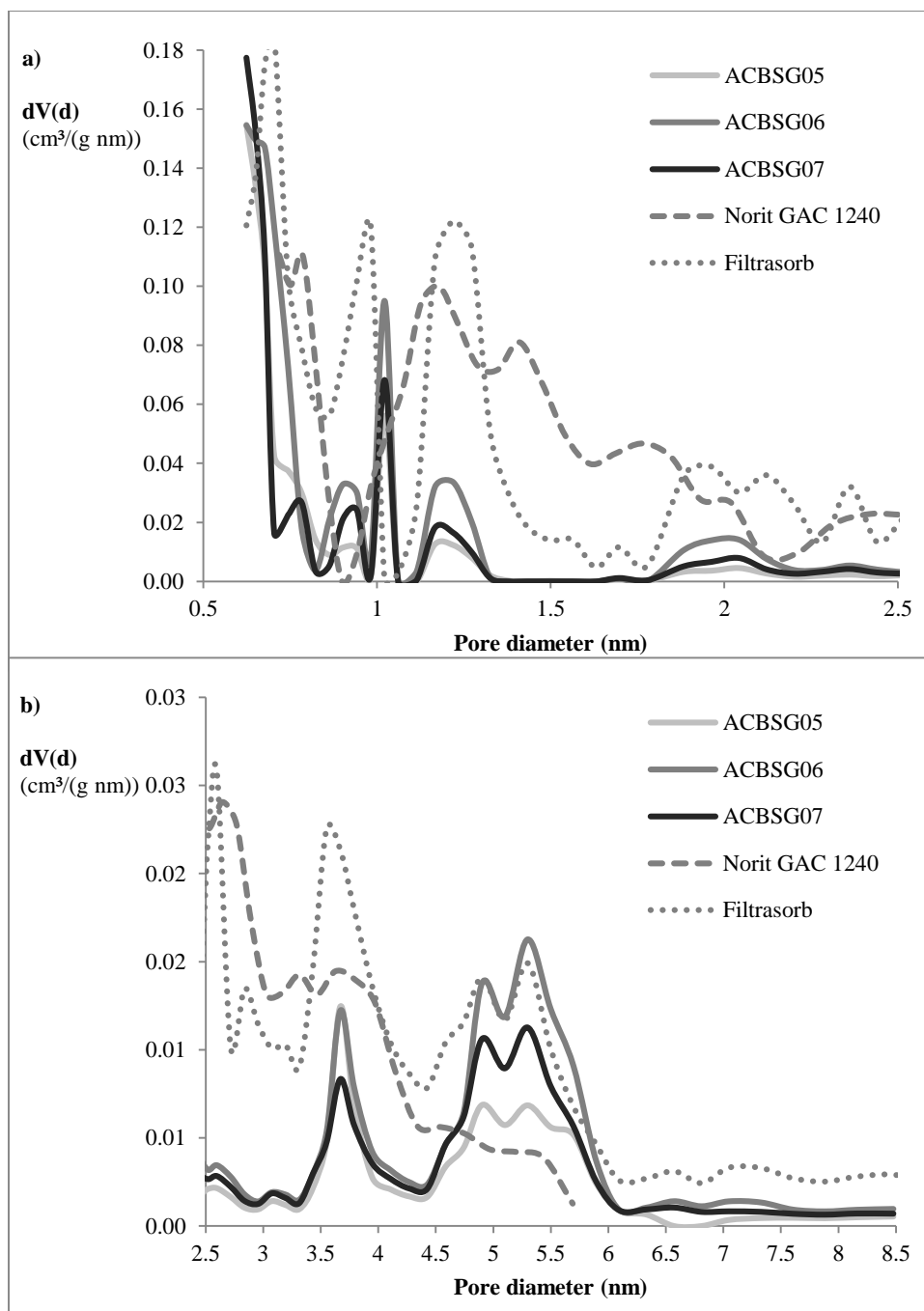
	$S_{BET}$ (m <sup>2</sup> /g)	$S_{micro}$ (m <sup>2</sup> /g)	$S_{ext}$ (m <sup>2</sup> /g)	$V_T$ (cm <sup>3</sup> /g)	$V_{Micro}$ (cm <sup>3</sup> /g)	$V_{Meso}$ (cm <sup>3</sup> /g)	$L_0$ (nm)	$E_0$ (kJ/mol)
<b>ACBSG05</b>	<b>686</b>	<b>422</b>	<b>100</b>	<b>0.335</b>	<b>0.274</b>	<b>0.060</b>	<b>0.9</b>	<b>23.5</b>
<b>ACBSG06</b>	<b>836</b>	<b>506</b>	<b>151</b>	<b>0.439</b>	<b>0.342</b>	<b>0.097</b>	<b>1.3</b>	<b>19.9</b>
<b>ACBSG07</b>	<b>758</b>	<b>461</b>	<b>121</b>	<b>0.382</b>	<b>0.304</b>	<b>0.078</b>	<b>1.0</b>	<b>22.2</b>
<b>Norit GAC 1240</b>	<b>1468</b>	<b>532</b>	<b>725</b>	<b>0.827</b>	<b>0.599</b>	<b>0.228</b>	<b>2.6*</b>	<b>15.5</b>

<b>Filtrisorb F400</b>	<b>1483</b>	<b>833</b>	<b>432</b>	<b>0.859</b>	<b>0.604</b>	<b>0.256</b>	<b>2.6*</b>	<b>15.5</b>
----------------------------	-------------	------------	------------	--------------	--------------	--------------	-------------	-------------

\* The empirical correlation (Stoeckli formula) is only valid for  $L_0$  values between 0.5 and 2.0 nm

149 For the ACs from BSG, the BET surface increases with increasing activation (from  
 150 ACBSG05 to ACBSG07 and to ACBSG06). The obtained BET surface for the ACs from  
 151 BSG is around half (686 – 836 m<sup>2</sup>/g) of the BET surface from the commercial ACs (1468  
 152 -1483 m<sup>2</sup>/g). Higher and longer activation times increase the BET surface, micropore  
 153 ( $V_{Micro}$ ), mesopore ( $V_{Meso}$ ) and the overall pore volumes ( $V_T$ ) of all the samples. The  
 154  $V_{Micro}/V_T$  ratio decreased from 0.81 to 0.78, indicating that the mesopores gain a larger  
 155 contribution to the total pore volume by increasing activation. This is also observed in the  
 156 broadening of the average micropore diameter ( $L_0$ ). In contrast to the commercial ACs, the  
 157 ACBSGs have average pore diameter that is 2 times smaller than the commercial ACs.  
 158 A rough estimation of the pore size distribution of the micropores (**Fig. 1**) is determined  
 159 by means of the Density Functional Theory (DFT). The pore size distribution reveals that  
 160 the ACBSGs consist of primarily pores with a diameter between 1 and 1.1 nm, followed  
 161 by two secondary micropores 0.82 – 0.97 nm and 1.12 – 1.32 nm. In addition wider  
 162 micropores are found of about 2 nm. The pore size distribution in the mesopore range  
 163 shows four peaks: at 3.7 nm, 4.9 nm, 5.3 nm and 5.8 nm respectively. An increase in  
 164 temperature and activation increases the amount of micropores and mesopores, without  
 165 increasing their size. When comparing with the pore size distribution of the commercial  
 166 ACs, a very discrete distribution is obtained by the activation and pyrolysis of BSG.





167

168

169 **Fig. 1** Pore size distribution of the ACs determined by DFT method for a) micropores; b)  
 170 mesopores (2.5 – 8.5 nm)

171 Prussian Blue (PB) was fixed on the surface of each of these five ACs to create an AC-PB  
 172 combination to enhance the adsorption capacity. Therefore, 1 g of AC was mixed with 150  
 173 mL of saturated PB solution and shaken for 48 hours. The pH of the solution was set at 7,

174 to prevent dissociation of the PB in an acidic or basic environment [44,45]. The AC was  
175 then filtered off using ashless Whatman filters, washed with water and dried at  $105 \pm 5$  °C  
176 for 24 h. The PB concentration of the solution before and after adsorption was obtained  
177 indirectly by measuring the iron concentration in the solutions using ICP-AES (Optima  
178 3300 DV, Perkin Elmer, Massachusetts, USA)-. The mass difference of PB was supposed  
179 to be bound to the AC. The mass of PB adsorbed on the surface of the AC is an important  
180 parameter to determine the extra amount of Cs that can be adsorbed. Both 5 ACs and 5  
181 AC-PBs were used in the batch adsorption experiments.

182 **Table 2** displays the mass of PB adsorbed on the AC expressed in  $\text{mg g}^{-1}$ . The observed  
183 differences in adsorbed amount might be related to the pore size distribution, allowing PB  
184 to move more freely in Norit GAC 1240, Filtrasorb 400 and ACBSG06. The latter was  
185 activated in the most severe conditions ( $850$  °C/45 min/15 mL), which led to an increase  
186 in overall pore sizes, as described above, increasing the mobility of the colloidal PB  
187 molecules.[46]

188 **Table 2** Mass of PB adsorbed on the five different activated carbons used in this study

Type of AC	mg PB $\text{g}^{-1}$ AC
Norit GAC 1240-PB	$13.9 \pm 0.1$
Filtrasorb 400-PB	$10.1 \pm 0.1$
ACBSG05-PB	$1.6 \pm 0.1$
ACBSG06-PB	$15.3 \pm 0.1$
ACBSG07-PB	$3.3 \pm 0.1$

## 189 **2.2 Solutions**

190 In order to be able to monitor the behaviour of Cs in these experiments, a  $1000 \text{ mg L}^{-1}$   
191  $\text{CsNO}_3$  standard solution was irradiated for 21 hours in the neutron flux of BR-1 at  
192 SCK·CEN ( $\varphi=3 \cdot 10^{11} \text{ n cm}^{-2} \text{ s}^{-1}$ ,  $\sigma=30 \cdot 10^{-24} \text{ cm}^{-2}$ ) to activate part of the Cs to  $^{134}\text{Cs}$ . The  
193  $^{134}\text{Cs}$  in the irradiated solution served as a tracer for the total Cs. The undiluted solution  
194 had an activity concentration of  $50.93 \pm 0.74 \cdot 10^3 \text{ Bq g}^{-1}$ . The radiopurity of it was checked  
195 by measuring it on a HPGe detector. No impurities could be identified.

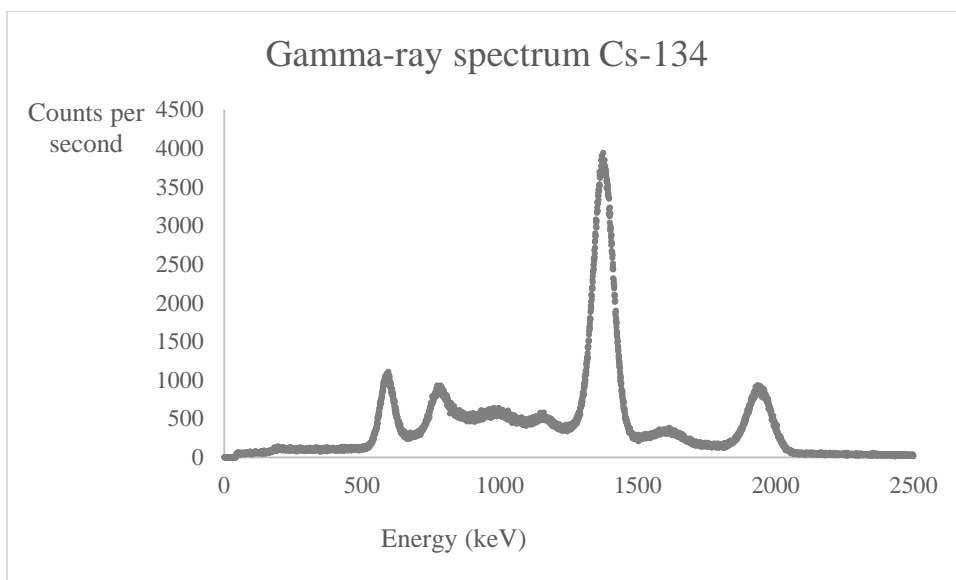
196 The solution was diluted to approximately 1:1000 in three steps. Dilution factors were  
197 determined gravimetrically and checked by measuring the activity of  $^{134}\text{Cs}$  in the solution  
198 using an ionisation chamber and a well-type NaI(Tl) detector.

199 Previous work showed that the  $\text{pH}_{\text{PZC}}$  of AC from BSG ranges from 10.6 to 10.8, and those  
200 of the used commercially available ACs from 11.5–11.7 [27]. Therefore the pH of the  
201 working solutions was adjusted to 7, 10 and 12 using ammonia. These working solutions  
202 had a  $^{134}\text{Cs}$  activity concentration of  $59.24 \pm 0.70$ ,  $59.67 \pm 0.70$ ,  $60.44 \pm 0.71 \text{ Bq g}^{-1}$   
203 corresponding to a Cs concentration of 1.16, 1.17 and 1.19  $\text{mg L}^{-1}$  at pH 7, 10 and 12,  
204 respectively.

### 205 **2.3 Gamma-ray spectrometry**

206 The activity of the samples was determined by  $4\pi$  gamma counting using a 20 x 20 cm  
207 NaI(Tl) well-type detector with a well-diameter of 25.4 mm and well-depth of 134.0 mm.  
208 In the NaI(Tl) well detector all the signals above the lower energy threshold of 50 keV  
209 were counted. All measurement results were corrected for background and decay. The total  
210 efficiency of the well-type NaI(Tl) detector was calculated using Monte Carlo simulations  
211 with the EGSnrc-code. The calculations were done using the same lower threshold of 50  
212 keV. Furthermore, the different filling heights of solution in the used centrifuge tubes were  
213 individually modelled. The calculated efficiencies were close to 100 % and showed a  
214 variation smaller than 1 % between empty and completely filled tubes.

215 A gamma-ray spectrum of the  $^{134}\text{Cs}$  solution obtained with the well-type NaI(Tl) detector  
216 is displayed in **Fig. 2**. The lower energy threshold of 50 keV is clearly visible. The spectrum  
217 shows the transitions at 605 keV ( $p=98.21$ ,  $\gamma_{1,0}$ ) and 796 keV ( $p=85.73$ ,  $\gamma_{3,1}$ ) [47]. The peak  
218 at 1401 keV is the sum peak of these transitions, caused by the simultaneous detection of  
219 both gamma rays. At 1970 keV the gamma rays of 569, 605 and 796 are collected  
220 simultaneously.



221  
222 **Fig. 2** Gamma-ray spectrum of a  $^{134}\text{Cs}$  solution measured in the well-type Na(Tl) detector

223 **2.4 Batch adsorption experiment**

224 The batch adsorption experiments were conducted using all 10 types ACs, i.e. 5 ACs both  
225 with and without fixed PB. Each of these ten ACs was tested for adsorption using three  
226  $^{134}\text{Cs}$  solutions of different initial pH (7-10-12) and similar activity.

227 Between 20 and 30 mg of AC and approximately 9 mL of Cs solution (approximately 60  
228  $\text{Bq g}^{-1}$   $^{134}\text{Cs}$ , corresponding to  $1.2 \text{ mg L}^{-1}$  Cs) at the desired initial pH (7, 10 or 12) were  
229 gravimetrically added into different centrifuge tubes (VWR High Performance 15 ml,  
230 VWR International, Leuven, Belgium). After shaking the tubes for 48 h in a Maxi-Mix III  
231 Vortex Mixer (Thermo Scientific, USA), each solution was filtered through a 75 mm funnel  
232 (VITLAB, GroBostheim, Germany) with an ashless Whatman filter and the filtrated  
233 solution was stored in a second centrifuge tube. The filter containing the AC was dried and  
234 stored in a third centrifuge tube. All three centrifuge tubes (the empty centrifuge tube, the  
235 filtered solution and filter paper with AC) were measured in the well-type NaI(Tl) detector.  
236 This test was conducted in triplo for each type of AC. Adsorption capacities at equilibrium  
237 ( $q_e$ , in mg/g) were calculated as follows:

238 
$$q_e = A_{\text{filter}} k_{\text{ac}} / m_{\text{AC}}. \quad (1)$$

239 Where  $A_{\text{filter}}$  is the measured activity in the filter (in Bq),  $k_{\text{ac}}$  is the recalculation constant for  
240 activity to mass (in mg/Bq) and  $m_{\text{AC}}$  is the mass of the AC used (in g).

241 To prove there were no losses of  $^{134}\text{Cs}$  during the experiment, a recovery experiment was  
242 set up. This experiment was conducted in exactly the same way prior to the batch  
243 adsorption experiment. Recovery rates were calculated for three ACs as the ratio between  
244 the activity of the solution in the centrifuge tube prior to shaking and the sum of the  
245 activities measured in the three centrifuge tubes after the adsorption experiment. A  
246 maximum of 0.7 % deviation from 100 % was found, indicating that the losses of activity  
247 throughout the adsorption procedure were minor.

## 248 **2.5 Single column experiment**

249 Adsorption of Cs on AC can be applied to both surface water (neutral to slightly acidic  
250 environment) and liquid waste treatment in decontamination units, where pH conditions  
251 can be more extreme. In order to test samples resembling the conditions described above  
252 and to find an optimal pH to promote column adsorption, solutions of different pH were  
253 tested: one acidic, one neutral and 2 basic. As a reference AC, Norit GAC 1240 was chosen  
254 for this experiment. Bio-rad Poly-Prep Chromatography Columns (0.8 x 4 cm) (Bio-Rad,  
255 California, USA) were filled with approximately 0.7 g of Norit GAC 1240 and pre-wetted  
256 with water. 11 mL of approximately  $37 \text{ Bq g}^{-1} \text{ }^{134}\text{Cs}$  solution at pH 4, 7, 10 and 12 was  
257 poured over these columns and collected, by gravity, in a centrifuge tube. The activity of  
258 the collected solution, as well as the activity remaining in the empty centrifuge tube, were  
259 both measured in the well-type detector. The collected solution was then poured over the  
260 column again. This cycle was repeated five times. Each test was conducted in duplo. After  
261 five cycles the column was measured in the well-type detector after air drying for 48 hours.  
262 Adsorption capacities ( $q$ ) were calculated as mg Cs (calculated from the column activity)  
263 per gram of AC.

264 On the basis of the first tests the most effective pH was determined, 5 different ACs (Norit  
265 GAC 1240, Filtrasorb 400, ACBSG05, ACBSG06, ACBSG07) were used in order to  
266 compare their performance. The column adsorption procedure was identical to the one  
267 described above. It was performed using 11 mL of approximately  $37 \text{ Bq g}^{-1} \text{ }^{134}\text{Cs}$  solution  
268 at pH 7.

269 For the column adsorption experiment a recovery experiment was also conducted. For this  
270 purpose, two columns filled with approximately 0.7 g of AC (Norit GAC 1240 and  
271 ACBSG07) were used. 11 mL of containing approximately  $37 \text{ Bq g}^{-1}$  of  $^{134}\text{Cs}$  was then

272 poured over each column and collected in a centrifuge tube. This process was repeated 5  
 273 times. The centrifuge tubes and column were measured as described above. The average  
 274 recovery rate showed no loss during the column test.

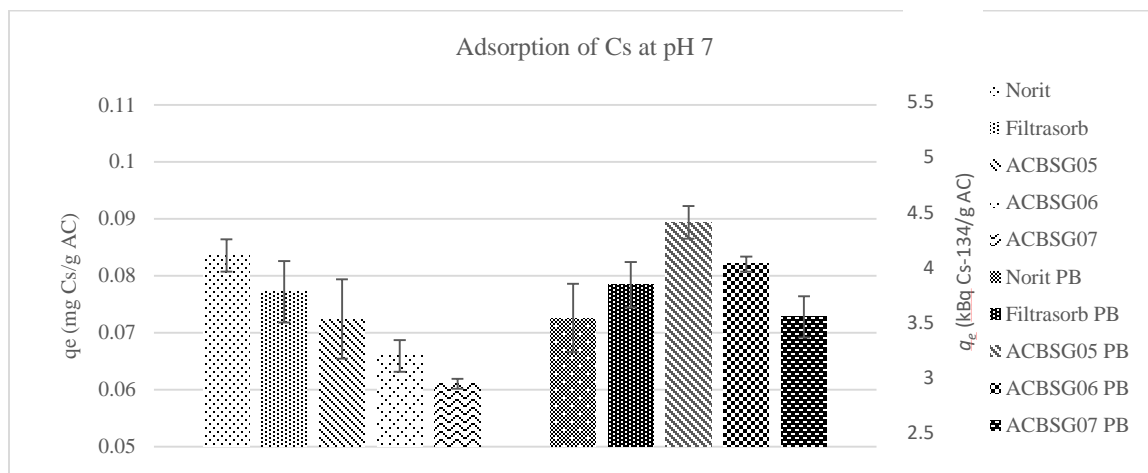
### 275 2.6 Sequential column experiment

276 In this part of the experiment five columns were filled with approximately 0.7 g of Norit  
 277 GAC 1240. 12 mL of approximately 37 Bq g<sup>-1</sup> Cs solution at pH 7 was poured over the  
 278 column and collected. After measuring the collected solution, it was poured successively  
 279 over the four remaining identical columns and the activity of the solution was measured  
 280 after each filtration. This test was conducted in duplo.

## 281 3. Results and discussion

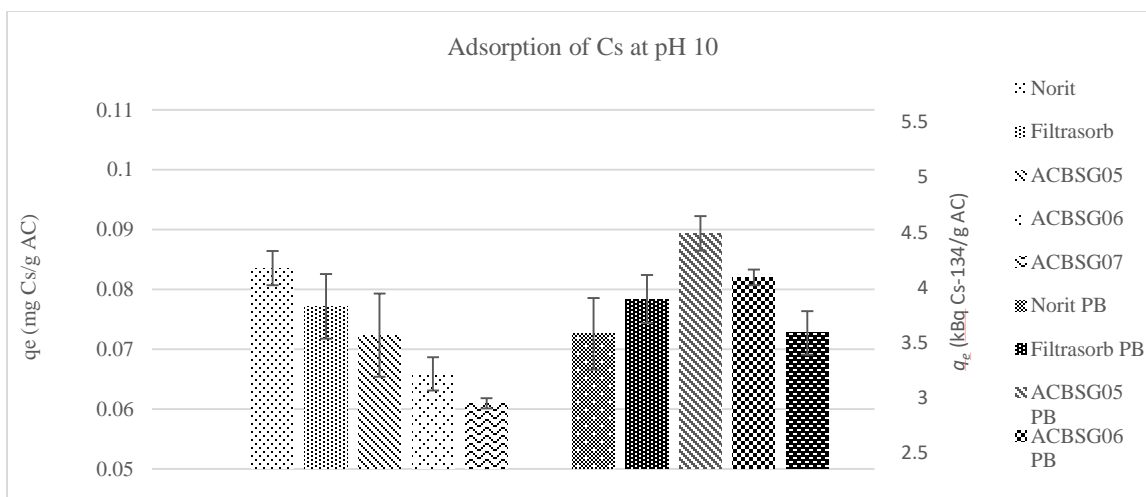
### 282 3.1 Batch adsorption experiment

283 Batch adsorption tests using different ACs could reveal the difference between the  
 284 commercial ACs and the AC from BSG. The influence of PB adsorption prior to Cs  
 285 adsorption and the influence of pH on the amount of adsorbed Cs were also determined.



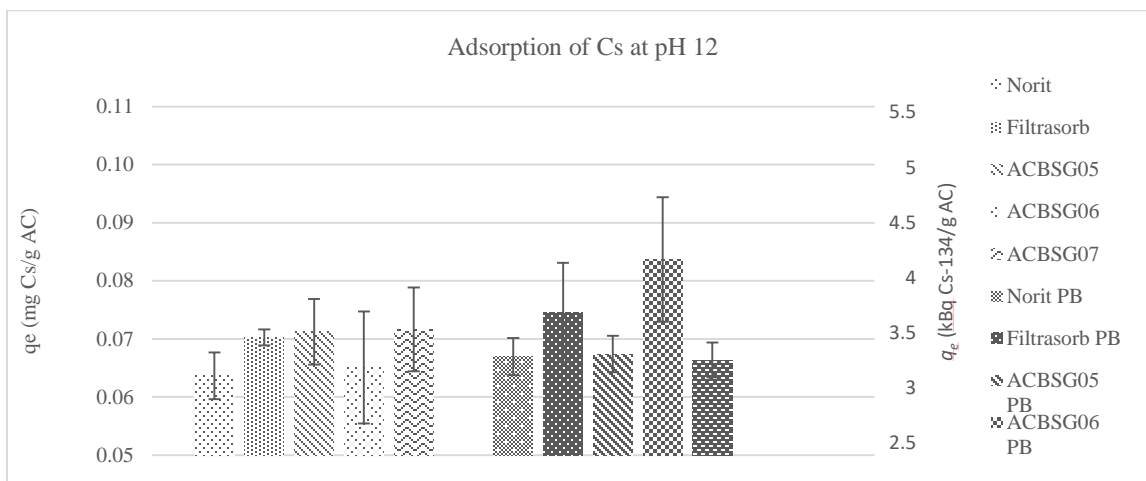
286  
 287

**Fig. 3** Adsorption capacities ( $q_e$ ) of Cs on different ACs during batch adsorption at pH 7



288  
289

**Fig. 4** Adsorption capacities ( $q_e$ ) of Cs on different ACs during batch adsorption at pH 10



290

**Fig. 5** Adsorption capacities ( $q_e$ ) of Cs on different ACs during batch adsorption at pH 12

292 The results of the batch adsorption experiments are displayed in **Fig. 3-5**. The untreated  
 293 ACs are plotted on the left and the ACs with PB adsorbed on the right side. Error bars show  
 294 the combined standard uncertainty. Statistical measurement uncertainties were calculated  
 295 and proven to be insignificant compared to the standard deviations between the 3 different  
 296 repeats of the experiments. For each pH the average activity concentrations and Cs  
 297 concentrations before and after adsorption are displayed in **Table 3**. The average removal  
 298 percentage is displayed at the different pH settings. Adsorption capacity at equilibrium is  
 299 expressed as  $q_e$  (mg Cs adsorbed per gram AC).

pH	Activity concentration before	Cs concentration before	Activity concentration after	Cs concentration after	Removal percentage
----	-------------------------------	-------------------------	------------------------------	------------------------	--------------------

	adsorption (Bq g <sup>-1</sup> )	adsorption (mg L <sup>-1</sup> )	after adsorption (Bq g <sup>-1</sup> )	adsorption (mg L <sup>-1</sup> )	
7	59.24 ± 0.70	1.16 ± 0.01	48.63 ± 1.86	0.95 ± 0.04	18.3 ± 3.0
10	59.67 ± 0.70	1.17 ± 0.01	47.11 ± 1.25	0.93 ± 0.02	21.0 ± 1.7
12	60.44 ± 0.71	1.19 ± 0.01	49.24 ± 1.18	0.96 ± 0.02	18.5 ± 1.2

300 **Table 3** Average measured (activity) concentrations before and after batch adsorption with  
301 calculated average removal for each tested pH

302 The best adsorption capacity ( $q_e$ ) was obtained at pH 10, although the differences between  
303 adsorption of solutions of different pH were not significant. At pH 12, all ACs were  
304 negatively charged, but this did not increase the adsorption of Cs on the AC. This may have  
305 been caused by the competition of adsorption between Cs and the high amount of ammonia  
306 present in the solution. The binding of PB on AC prior to Cs adsorption did not significantly  
307 promote the adsorption at any of the tested pH values. Furthermore the dissociation of  
308 unbound PB happens above pH 8. This can explain the fact that AC with PB shows the  
309 same  $q_e$  values at pH 10 and 12 as for the unloaded AC. This experiment shows that the  
310 ACs have similar adsorption capacities in different circumstances. A removal of about 20  
311 % is limited compared to the results obtained by ion exchangers, where removal rate of  
312 above 70 % are easily reached [48,16]. Some manuscripts report extremely low [39,49]  
313 removal percentages for Cs using AC. Kimura et al. [15] reported removal percentages up  
314 to almost 100 %, but used AC dosages were approximately 30 times higher than in this  
315 manuscript. The ACs investigated seem to have an interesting affinity for Cs, even at lower  
316 dosage.

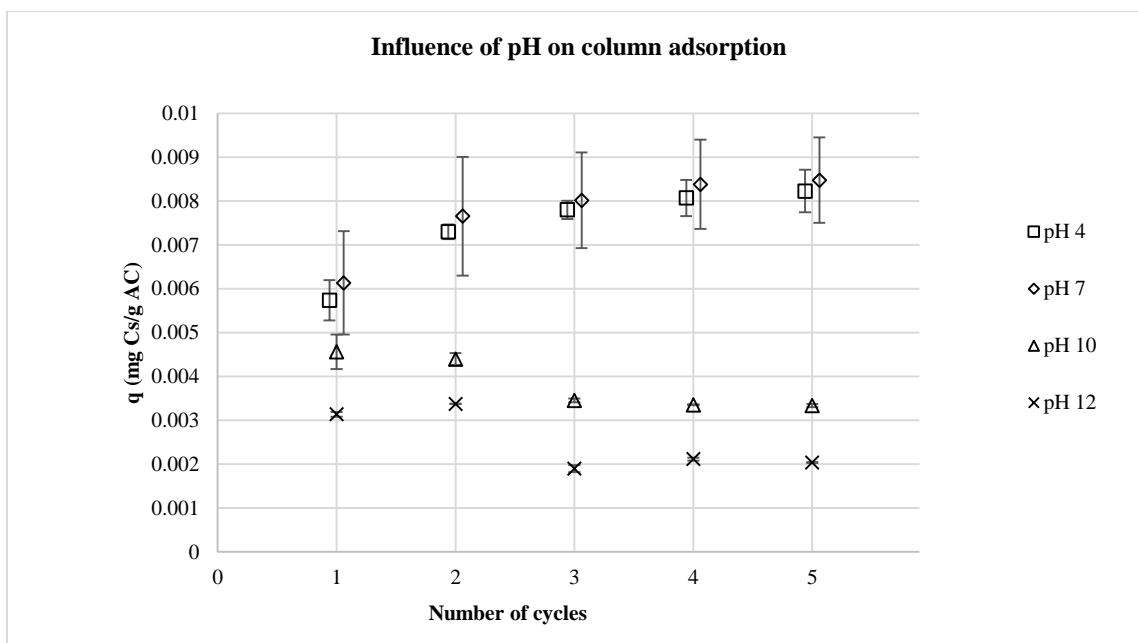
### 317 **3.2 Single column adsorption**

#### 318 **3.2.1 pH selection**

319 Results of the column filtration of solution at different pH (4-7-10-12) are shown in **Fig.**

320 **6.**

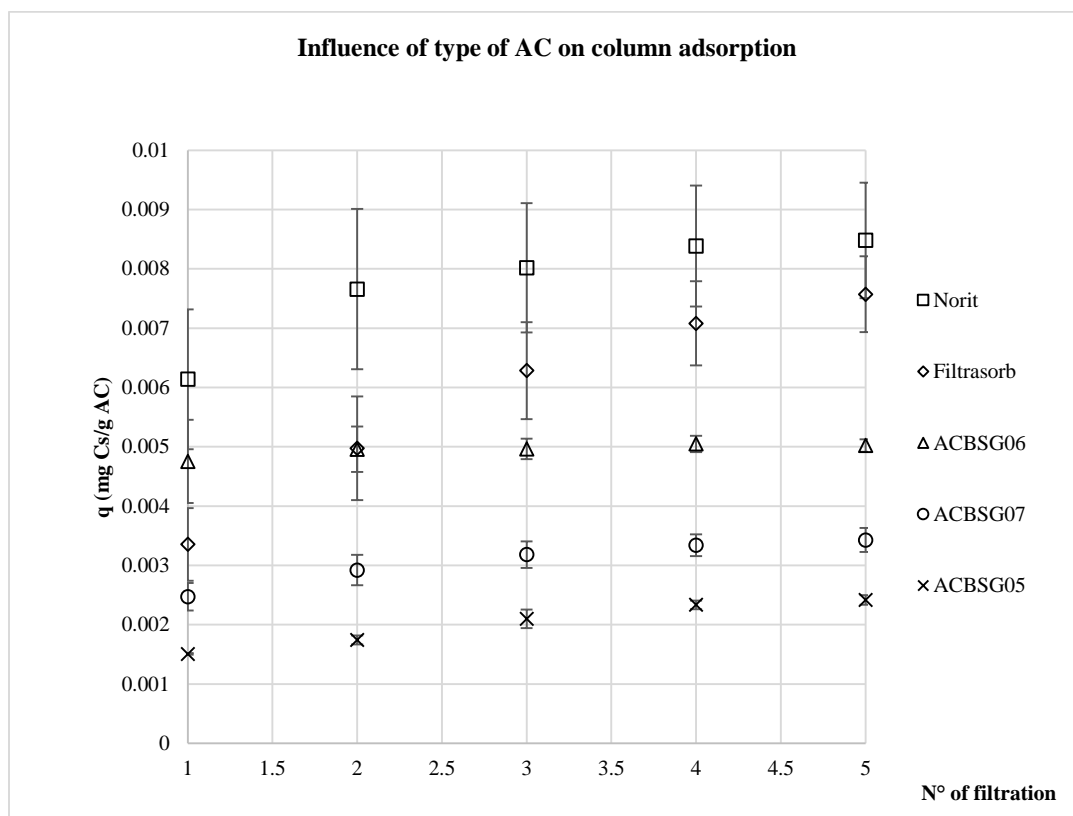




321  
 322 **Fig. 6** Adsorption capacities after 5 cycles of adsorption on a column filled with Norit GAC  
 323 1240 using solutions with different pH. Data points have been artificially separated to  
 324 enhance visibility.

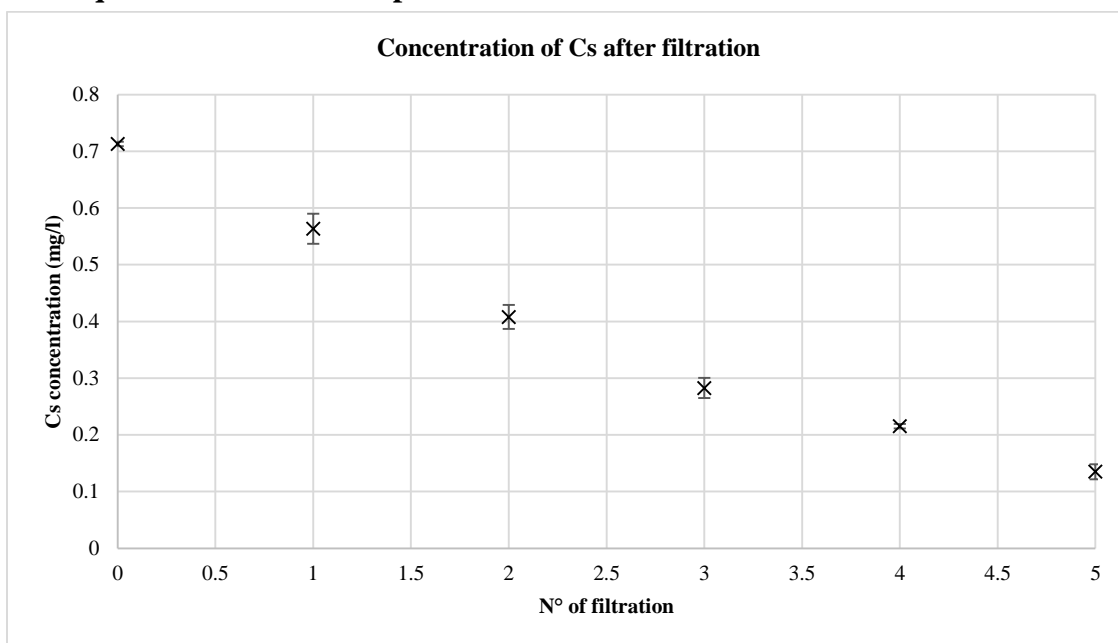
325 For pH 4 and pH 7, the adsorption capacity ( $q$ ) increased with each cycle with a maximum  
 326  $q_e$  of about  $0.0083 \text{ mg g}^{-1}$  Cs on Norit GAC 1240. A higher pH drastically lowered the  
 327 maximum adsorbed amount of Cs on the AC, to a  $q_e$  of  $0.0033 \text{ mg g}^{-1}$  at pH 10 and  $0.0020$   
 328  $\text{mg g}^{-1}$  at pH 12 after 5 cycles. Additionally  $q$  seems to decrease with each additional cycle.  
 329 This effect was probably due to the competition of adsorption by the ammonia ion in the  
 330 solutions, which explains why the lowest adsorbed amount is found at the highest pH. The  
 331 competition between Cs and the ammonia ion may wash out the Cs already adsorbed on  
 332 the AC, decreasing  $q$  after three cycles. A neutral to slightly acidic environment enhances  
 333 Cs adsorption in comparison to a strongly basic environment.

## 334 3.2.2 AC selection



335  
336 **Fig. 7** Adsorption capacities after 5 cycles of adsorption on 5 ACs using a solution of pH  
337 7

338 The commercial ACs show a significantly higher adsorption capacity  $q$  of Cs compared to  
339 the ACBSGs. Norit GAC 1240 reached its equilibrium adsorption capacity ( $q_e$  of 0.0085  
340  $\text{mg g}^{-1}$ ) after 4 cycles, while  $q$  on Filtrasorb 400 still rose to 0.0075  $\text{mg g}^{-1}$  after 5 cycles.  
341 Both commercial ACs are in granular form, making a better interaction between the surface  
342 of the AC and the Cs solution possible compared to the three ACBSGs, having a smaller  
343 particle size. The ACBSGs tended to stick together in the column with air still present in  
344 open spaces, causing possible channel formation. This resulted in a less efficient interaction  
345 between AC surface and solution. Additionally, this caused a limited contact time and  
346 smaller contact area for the ACBSGs. All 3 ACBSGs reached their equilibrium adsorption  
347 capacities after 2-3 cycles. ACBSG06 performed better compared to ACBSG05 and  
348 ACBSG07 (a  $q$  of 0.0050  $\text{mg g}^{-1}$ , compared to 0.0024  $\text{mg g}^{-1}$  and 0.0034  $\text{mg g}^{-1}$   
349 respectively), possibly due to the higher activation temperature used, creating a slightly  
350 wider pore distribution thus increasing the mobility of the Cs ions in aqueous solutions.

351 **3.4 Sequential column adsorption**

352 **Fig. 8** Decrease in Cs concentration after sequential column adsorption with Norit GAC  
 353 1240 GAC1240  
 354

355 Passing the solution through five columns filled with Norit GAC 1240 decreased the  
 356 concentration from  $36.3 \pm 0.3 \text{ Bq g}^{-1}$  ( $0.713 \text{ mg L}^{-1}$  Cs) to  $6.8 \pm 0.9 \text{ Bq g}^{-1}$  ( $0.135 \text{ mg L}^{-1}$   
 357 Cs). For this test, the decrease showed a removal rate of  $28.1 \pm 2.8 \%$  of the initial Cs  
 358 concentration per filtration. This result indicated that further removal of low levels of Cs  
 359 is possible using sequential filtration steps. No equilibrium was reached during this  
 360 experiment, as displayed in **Fig. 8**.

361 **Conclusions**

362 This work studied the removal of low concentrations of Cs from aqueous solutions by AC.  
 363 For measurement,  $^{134}\text{Cs}$  served as a tracer for the total Cs concentration. A standard  
 364 solution of Cs was irradiated in a neutron flux to provide a radiopure  $^{134}\text{Cs}$  solution of  
 365 which both the exact concentration of Cs and activity of the  $^{134}\text{Cs}$  tracer were known. Batch  
 366 experiments using a variety of ACs adsorbing Cs from solutions with different pH showed  
 367 no significant difference between the adsorption capacities at equilibrium for Cs (expressed  
 368 as  $q_e$  values in mg Cs per gram AC) on either commercial AC or AC from BSG. Also the

369 difference in adsorption between the Cs solutions of different pH was not significant.  
370 Binding PB on the ACs prior to the adsorption of Cs showed no significant effect on the  $q_e$   
371 for any of ACs. Because batch experiments revealed no difference between the ACs,  
372 column experiments were conducted. A column experiment with Norit GAC 1240 using 4  
373 solutions with a different pH showed that a neutral to slightly acidic pH increased the  
374 adsorption of Cs. At a higher pH the effect of the competition with ammonia ions caused  
375 a decrease of  $q_e$ . For the lab-scale ACs the ACBSG06 (the AC activated at the highest  
376 temperature) reached the highest  $q_e$ . Both commercially available ACs (Filtrisorb 400 and  
377 Norit GAC 1240) had even higher  $q_e$  values. This was caused by the difference in physical  
378 properties of the AC. Using sequential column adsorption to remove low concentrations of  
379 Cs from aqueous solutions led to promising results, as a steady removal rate per cycle step  
380 was observed. An equilibrium state is expected to be reached after several stages, where  
381 further removal is ineffective. A study will be performed to confirm this. The experiment  
382 showed that AC has potential as a low-cost and effective adsorbent for removal of low Cs  
383 concentrations. Removal percentages and adsorption capacities were comparable or higher  
384 than in relevant literature. Feasibility studies on the application of the method described in  
385 this paper in the nuclear industry are planned to be conducted.

## 386 **Acknowledgements**

387 This work was supported by the European Commission within HORIZON2020 via the  
388 EURATOM Project EUFRAT. The authors would also like to thank Prof. Vera Meynen  
389 from the Department of Chemistry, Laboratory for Adsorption and Catalysis, University  
390 Antwerp, Belgium.

## 391 **References**

392 1. Whicker FW, Kaplan DI, Jr. CTG, Hamby DM, Higley KA, Hinton TG, Rowan DJ,  
393 Schreckhise RG (2007) Cesium-137 in the Environment: Radioecology and Approaches to  
394 Assessment and Management. NCRP Book No. 154 National Council on Radiation  
395 Protection and Measurements. Bethesda,

- 396 2. Steinhäuser G, Brandl A, Johnson TE (2014) Comparison of the Chernobyl and  
397 Fukushima nuclear accidents: A review of the environmental impacts. *Science of The Total*  
398 *Environment* 470–471 (0):800-817. doi:<http://dx.doi.org/10.1016/j.scitotenv.2013.10.029>  
399 3. TEPCO (2013) Detailed analysis results in the port, discharge channel and bank  
400 protection at Fukushima Daiichi NPS (As of August 28).
- 401 4. Lestaevel P, Racine R, Bensoussan H, Rouas C, Gueguen Y, Dublineau I, Bertho J-M,  
402 Gourmelon P, Jourdain J-R, Souidi M (2010) Césium 137 : propriétés et effets biologiques  
403 après contamination interne. *Médecine Nucléaire* 34:108-118
- 404 5. PHS (2004) Toxicological profile for cesium. Agency for Toxic Substances and Disease  
405 Registry,
- 406 6. Kinoshita N, Sueki K, Sasa K, Kitigawa J-i, Ikarashi S, Nishimura T, Wong Y-S, Satou  
407 Y, Handa K, Takahashi T, Sato M, Yamagata T (2011) Assessment of individual  
408 radionuclide distributions from the Fukushima nuclear accident covering central-east  
409 Japan. *Proceedings of the national academy of sciences* 108:19526-21952
- 410 7. Liu X, Chen G-R, Lee D-J, Kawamoto T, Tanaka H, Chen M-L, Luo Y-K (2014)  
411 Adsorption removal of cesium from drinking waters: A mini review on use of biosorbents  
412 and other adsorbents. *Bioresource Technology* 160:142-149.  
413 doi:<http://dx.doi.org/10.1016/j.biortech.2014.01.012>
- 414 8. Li D, Kaplan DI, Knox AS, Crapse KP, Diprete DP (2014) Aqueous 99Tc, 129I and  
415 137Cs removal from contaminated groundwater and sediments using highly effective low-  
416 cost sorbents. *Journal of Environmental Radioactivity* 136 (0):56-63.  
417 doi:<http://dx.doi.org/10.1016/j.jenvrad.2014.05.010>
- 418 9. Ding D, Zhao Y, Yang S, Shi W, Zhang Z, Lei Z, Yang Y (2013) Adsorption of cesium  
419 from aqueous solution using agricultural residue - Walnut shell: Equilibrium, kinetic and  
420 thermodynamic modeling studies. *Water Research* 47:2563-2571
- 421 10. Lan T, Feng Y, Liao J, Li X, Ding C, Zhang D, Yang J, Zeng J, Yang Y, Tang J, Liu  
422 N (2014) Biosorption behavior and mechanism of cesium-137 on *Rhodosporidium fluviale*  
423 strain UA2 isolated from cesium solution. *Journal of Environmental Radioactivity* 134  
424 (0):6-13. doi:<http://dx.doi.org/10.1016/j.jenvrad.2014.02.016>
- 425 11. Parajuli D, Tanaka H, Hakuta Y, Minami K, Fukuda S, Umeoka K, Kamimura R,  
426 Hayashi Y, Ouchi M, Kawamoto T (2013) Dealing with the aftermath of Fukushima  
427 Daiichi nuclear accident: decontamination of radioactive cesium enriched ash. *Environ Sci*  
428 *Technol* 47 (8):3800-3806. doi:10.1021/es303467n
- 429 12. Ding D, Lei Z, Yang Y, Feng C, Zhang Z (2014) Selective removal of cesium from  
430 aqueous solutions with nickel (II) hexacyanoferrate (III) functionalized agricultural  
431 residue–walnut shell. *Journal of Hazardous Materials* 270:187-195
- 432 13. Haas PA (1993) A review of information on ferrocyanide solids for removal of cesium  
433 from solutions. *Separation science and technology* 28 (1):2479-2506
- 434 14. Ding D, Zhang Z, Lei Z, Yang Y, Cai T (2015) Remediation of radiocesium-  
435 contaminated liquid waste, soil, and ash: a mini review since the Fukushima Daiichi  
436 Nuclear Power Plant accident. *Environmental Science and Pollution Research* 23 (3):2249-  
437 2263. doi:10.1007/s11356-015-5825-4
- 438 15. Kimura K, Hachinohe M, Klasson KT, Hamamatsu S, Hagiwara S, Todoriki S,  
439 Kawamoto S (2014) Removal of Radioactive Cesium from Low-Level Contaminated  
440 Water by Charcoal and Broiler Litter Biochar. *Food Science and Technology Research* 20  
441 (6):1183-1189. doi:10.3136/fstr.20.1183

- 442 16. Parab H, Sudersanan M (2010) Engineering a lignocellulosic biosorbent – Coir pith for  
443 removal of cesium from aqueous solutions: Equilibrium and kinetic studies. *Water*  
444 *Research* 44 (3):854-860. doi:<http://dx.doi.org/10.1016/j.watres.2009.09.038>
- 445 17. Ofomaja AE, Pholosi A, Naidoo EB (2015) Application of raw and modified pine  
446 biomass material for cesium removal from aqueous solution. *Ecological Engineering*  
447 82:258-266. doi:<http://dx.doi.org/10.1016/j.ecoleng.2015.04.041>
- 448 18. Mohan DP, C.U. Jr. (2006) Activated carbons and low cost adsorbents for remediation  
449 of tri- and hexavalent chromium from water. *Journal of Hazardous Materials (B137)*:762-  
450 811
- 451 19. Marsh H, Rodríguez-Reinoso F (2006) Activated carbon. Elsevier Science &  
452 Technology books,
- 453 20. Montana MC, A.; Serrano, I.; Devesa, R.; Matia, L.; Vallés, I. (2013) Removal of  
454 radionuclides in drinking water by membrane treatment using ultrafiltration, reverse  
455 osmosis and electro dialysis reversal. *Journal of Environmental Radioactivity*
- 456 21. Biniak S, Szymanski G, Siedlewski J, Swiatkowski A (1997) The characterization of  
457 activated carbons with oxygen and nitrogen surface groups. *Carbon* 35 (12):1799-1810
- 458 22. McKendry P (2002) Energy production from biomass (part 2): conversion technologies.  
459 *Bioresource Technology* 83:47-54
- 460 23. Goyal HB, Seal D, Saxena RC (2008) Bio-fuels from thermochemical conversion of  
461 renewable resources: A review. *Renewable and Sustainable Energy Reviews* 12:504-517
- 462 24. Bansal RC, Goyal M (2005) Activated Carbon Adsorption. Taylor & Francis, Boca  
463 Raton
- 464 25. Menéndez-Díaz JA, Martín-Gullón I (2005) Types of carbon adsorbents and their  
465 production. In: T.J. B (ed) *Activated Carbon Surfaces in Environmental Protection*.  
466 Elsevier Ltd.,
- 467 26. Hameed BH, Rahman AA (2008) Removal of phenol from aqueous solutions by  
468 adsorption onto activated carbon prepared from biomass material. *Journal of Hazardous*  
469 *Materials* (160):576-581
- 470 27. Vanreppelen K, Vanderheyden S, Kuppens T, Schreurs S, Yperman J, Carleer R (2014)  
471 Activated carbon from pyrolysis of brewer's spent grain: Production and adsorption  
472 properties. *Waste Management & Research*
- 473 28. Tanthapanichakoon W, Ariyadejwanich P, Japthong P, Nakagawa K, Mukai SR,  
474 Tamon H (2005) Adsorption-desorption characteristics of phenol and reactive dyes from  
475 aqueous solution on mesoporous activated carbon prepared from waste tires. *Water*  
476 *Research* 39:1347-1353
- 477 29. Mussatto SI, Dragone G, Roberto IC (2006) Brewer's spent grain: generation,  
478 characteristics and potential applications. *Journal of Cereal Science* (43):1-14
- 479 30. Mahmood ASN, Brammer JG, Hornung A, Steele A, Poulston S (2013) The  
480 intermediate pyrolysis and catalytic steam reforming of Brewers spent grain. *Journal of*  
481 *Analytical and Applied Pyrolysis* 103:328-342
- 482 31. Yang G, Chen H, Qin H, Feng Y (2014) Amination of activated carbon for enhancing  
483 phenol adsorption: Effect of nitrogen-containing functional groups. *Applied Surface*  
484 *Science* 293:299-305
- 485 32. Bagreev A, Bashkova S, Bandoz TJ (2002) Adsorption of SO<sub>2</sub> on activated carbons:  
486 The effect of nitrogen functionality and pore siz. *Langmuir* 18 (4):1257-1264

- 487 33. Bagreev A, Menendez JA, Dukhno I, Tarasenko Y, Bandosz TJ (2004) Bituminous  
488 coal-based activated carbons modified with nitrogen as adsorbents of hydrogen sulfide.  
489 Carbon 42:469-476
- 490 34. Hayden RA (1995) Method for reactivating nitrogen-treated carbon catalysts. Google  
491 Patents,
- 492 35. Lorenc-Grabowska EG, G.; Diez, M.A. (2012) Kinetics and equilibrium study of  
493 phenol adsorption on nitrogen-enriched activated carbons. Fuel
- 494 36. Matzner SB, H.P. (1998) Influence of nitrogen doping on the adsorption and reduction  
495 of nitric oxide by activated carbon. Carbon 36 (11):1697-1709
- 496 37. Bandosz TJ, Ania CO (2006) Surface chemistry of activated carbons and its  
497 characterization. In: Bandosz TJ (ed) Activated Carbon Surfaces in Environmental  
498 Remediation. Elsevier, pp 159-229
- 499 38. Song K-C, Lee HK, Moon H, Lee KJ (1997) Simultaneous removal of the radiotoxic  
500 nuclides Cs137 and I129 from aqueous solution. Separation and Purification Technology  
501 12 (3):215-227. doi:[http://dx.doi.org/10.1016/S1383-5866\(97\)00045-2](http://dx.doi.org/10.1016/S1383-5866(97)00045-2)
- 502 39. Caccin M, Giacobbo F, Da Ros M, Besozzi L, Mariani M (2012) Adsorption of  
503 uranium, cesium and strontium onto coconut shell activated carbon. Journal of  
504 Radioanalytical and Nuclear Chemistry 297 (1):9-18. doi:10.1007/s10967-012-2305-x
- 505 40. Cabot Corporation - Safety HaEA (2015) Safety data sheet - Norit GAC 1240.
- 506 41. Carbon C (2015) Filtrasorb 400 - Granular Activated Carbon.
- 507 42. Mikhail RS, Brunauer S, Bodor EE (1968) Investigations of a complete pore structure  
508 analysis. Journal of Colloid and Interface Science 26 (1):45-53.  
509 doi:[http://dx.doi.org/10.1016/0021-9797\(68\)90270-1](http://dx.doi.org/10.1016/0021-9797(68)90270-1)
- 510 43. Klobes P, Meyer K, Munro RG (2006) Porosity and Specific Surface Area  
511 Measurements for Solid Materials. National Institute of Standards and Technology,  
512 Washington
- 513 44. Mohammad A, Yang Y, Khan MA, Faustino PJ (2015) Long-term stability study of  
514 Prussian blue-A quality assessment of water content and cyanide release. Clinical  
515 toxicology (Philadelphia, Pa) 53 (2):102-107. doi:10.3109/15563650.2014.998337
- 516 45. Ricci F, Palleschi G (2005) Sensor and biosensor preparation, optimisation and  
517 applications of Prussian Blue modified electrodes. Biosensors and Bioelectronics 21  
518 (3):389-407. doi:<http://dx.doi.org/10.1016/j.bios.2004.12.001>
- 519 46. Vanreppelen K (2016) Towards a circular economy – Development, characterisation,  
520 techno-economic analysis and applications of activated carbons from industrial rest  
521 streams. UHasselt, To be defended
- 522 47. Bé L-LC-M-M (2012) Table de Radionucléides - Cs 134.
- 523 48. Lalmunsiam, Lalhriatpuia C, Tiwari D, Lee S-M (2014) Immobilized nickel  
524 hexacyanoferrate on activated carbons for efficient attenuation of radio toxic Cs(I) from  
525 aqueous solutions. Applied Surface Science 321:275-282.  
526 doi:<http://dx.doi.org/10.1016/j.apsusc.2014.09.200>
- 527 49. Brown J, Hammond D, Wilkins BT (2008) Handbook for Assessing the Impact of a  
528 Radiological Incident on Levels of Radioactivity in Drinking Water and Risks to  
529 Operatives at Water Treatment Works: Supporting Scientific Report Oxfordshire

530